Carbohydrate Polymers 94 (2013) 874–881

Contents lists available at SciVerse ScienceDirect

Carbohydrate Polymers

journal homepage: www.elsevier.com/locate/carbpol

Plasticization effect of triacetin on structure and properties of starch ester film

Jie Zhu, Xiaoxi Li, Chen Huang, Ling Chen, Lin Li*

Ministry of Education Engineering Research Center of Starch & Protein Processing, Guangdong Province Key Laboratory for Green Processing of Natural Products and Product Safety, College of Light Industry and Food Sciences, South China University of Technology, Guangzhou 510640, China

ARTICLE INFO

Article history:
Received 27 November 2012
Received in revised form 13 February 2013
Accepted 14 February 2013
Available online 21 February 2013

Keywords:
Starch ester
Triacetin
Plasticizer
Interaction
Structure
Property

ABSTRACT

The aim of this work was to evaluate the plasticizing effect of triacetin on the structure and properties of starch ester film and further establish the structure–property relationships. The presence of triacetin resulted in multiple structure changes of the film. The mobility of macromolecular chain was increased to form scattered crystallite during the film formation process. The amorphous region was enlarged to contain more triacetin squeezed from crystalline region. The plasticization of triacetin and restriction of crystallite oppositely influenced the mobility of macromolecular chains in different regions. The thermal stability of triacetin changed along with its fluctuant interaction with macromolecules. Comparatively, the enhanced ether bond and the restriction from crystalline regions on the mobility of the amorphous chain consequently improved the thermal stability of the film matrix. The interaction between triacetin and starch ester was essential to film forming but unexpectedly lowered the triacetin stability.

1. Introduction

Starch is a potentially biodegradable material to replace the petroleum-based plastics in food packaging industry (Chandra & Rustgi, 1998; Siracusa, Rocculi, Romani, & Rosa, 2008; Viera, Da Silva, Dos Santos, & Beppu, 2011). The use of starch would consequently reduce the ecological problems caused by traditional plastics (Tharanathan, 2003; Siracusa et al., 2008). However, the huge water uptakes as well as the brittleness of starch-based material (Shogren, 1992) caused by the hydrophilic nature of starch are the major drawbacks and tremendous limitations in its application as food packaging. In order to improve the water-resistance, previous researchers have stated briefly that the esterification converts the hydrophilic native starch to hydrophobic starch ester efficiently, especially when the degree of substitution (*DS*) is high enough (Fringant, Rinaudo, Foray, & Bardet, 1998; Nejad, Ganster, & Volkert, 2010). However, the melting and the process temperatures of starch ester are still close to or higher than its degradation temperature (Nejad et al., 2010). In order to further overcome this issue, plasticizers are applied to increase the free volume or segmental molecular motion of polymers, shield the inter- and intra-macromolecular interactions and lower internal friction in the biopolymer material (Mathew & Dufresne, 2002; Matveev, Grinberg, & Tolstoguzov, 2000; Santosa & Padua, 1999; Suyatma, Tighzert, Copinet, & Coma, 2005). As a consequence, plasticizing effect decreases the melting and process temperature and thus facilitates the thermoplastic processing (Avérous & Halley, 2009; Mathew & Dufresne, 2002). In previous researches, triacetin has been proved to display effective plasticization for starch esters (Bonacucina et al., 2006; Fringant et al., 1998; Nejad et al., 2010; Nejad, Ganster, Bohn, Volkert, & Lehmann, 2011; Volkert, Lehmann, Greco, & Nejad, 2010). In addition, other chemical reagents, such as alkenyl succinic anhydrides and dicarboxylic acid diesters (Bonacucina et al., 2006; Rapthel, Wagner, & Kakuschke, 1998; Tarvainen et al., 2003) were also tested. Compared with the unplasticized starch esters films, the glass-rubber transition temperature (T_g) of plasticized films was reduced, and the mechanical properties were enhanced (Nejad et al., 2010, 2011).

Although the plasticization promotes the flexibility of starch esters film, previous studies rarely discussed the changes of the microstructure and crystalline structure of the film matrix during the film forming and storage. Moreover, some properties of starch ester films are still unqualified even after plasticization (Nejad et al., 2010), which still limits the application of such kind of biodegradable materials. Mathew and Dufresne (2002) have discussed that the aging through crystallization of thermoplastic starch, *i.e.* retrogradation, results from the reassociation during the storage of amorphous gelatinized starch or starch sample with a low degree of ordering into a more ordered state, which are both affected by the plasticizer. To the best of our knowledge so far, no

* Corresponding author. Tel.: +86 20 8711 3252; fax: +86 20 8711 3252.
E-mail addresses: zhujie2009@163.com (J. Zhu), felinli@scut.edu.cn (L. Li).

0144-8617/$ – see front matter © 2013 Elsevier Ltd. All rights reserved.
http://dx.doi.org/10.1016/j.carbpol.2013.02.020

Table 1
The molecular weight distribution of starch ester.

M_w (g/mol)	10,000–50,000	50,000–80,000	80,000–100,000	100,000–1000,000
Ratio (%)	53.87	21.91	7.06	17.90

straightforward relationship has been established between the structure and properties of plasticized starch esters film. Discussion about the interaction between plasticizer and starch ester molecules could be necessary for further understanding the effect of such component on the structure and properties of these materials.

In this paper, Fourier-transform infrared spectroscopy was used to investigate the interaction between triacetin and starch ester molecules. Scanning electron microscope, small and wide angle X-ray scattering, thermogravimetric analysis and dynamic mechanical analysis were performed to characterize the effect of triacetin on the morphology, microstructure, crystalline structure, thermal and mechanical properties of the film.

2. Materials and methods

2.1. Materials

Starch ester powder (DS = 2.49) made from native G50 (Penford, Australia), was prepared by acetyl esterification according to the method of our previous studies (Chen, Li, Li, & Guo, 2007; Pu et al., 2011). The average molecular weight (M_w) of this material is 69,910 (g/mol) as determined by gel permeation chromatography gel permeation chromatography (GPC; Waters Co., USA) combined with multi angle light scattering (MALS; Wyatt Technology Co., USA), and the molecular weight distribution is presented in Table 1. Triacetin (AR, M_w = 218.20) was purchased from Aladdin Chemistry Co. Ltd. (Shanghai, China).

2.2. Film preparation

Starch ester films were prepared by a solvent-cast method using acetone as the solvent. 2 g starch ester powder was dissolved in 50 g acetone. Triacetin was added in 0 wt% up to 30 wt% (w/w, total mass of the film). The mixture was stirred for 4 h and allowed for another 2 h stir after triacetin addition. The solution was then cast in a polypropylene mold (casting area.12 cm × 18 cm). The solvent was allowed to evaporate at 45 °C for 12 h. All the films were stored with resealable bags at the constant temperature (26 °C) and humidity (40%) for 24 h before analysis.

2.3. Scanning electron microscope (SEM) observation

The cross-section of the films were observed with a EVO 18 scanning electron microscope (Carl Zeiss Microscopy, LLC., Germany) operating at 20.0 kV high voltages. The specimens were frozen under liquid nitrogen and then fractured, mounted, coated with a thin gold film.

2.4. Fourier-transform infrared (FTIR) spectroscopy

The IR spectra of the films were determined using a Tensor 37 spectrometer (Bruker Optik, Germany) in attenuated total reflectance (ATR) mode between 600 and 4000 cm^{-1}, with 32 scans at a resolution of 4 cm^{-1}. Before film analysis, an open bean background spectrum of clean crystal was recorded. Three times of repetition were performed. Data analysis was performed with Peak Fit 4.12 (SYSTAT Software Inc., Richmond, CA, USA) program. AutoFit peaks III deconvolution method was applied. The deconvolution filter constant is 75 and was kept consistent for all samples.

2.5. Small and wide angle X-ray scattering (SAXS/WASX) experiment

The films were cut into strips (2 cm × 0.8 cm) for SAXS/WAXS experiment using a SAXSess camera (Anton-Paar, Graz, Austria). A PW3830 X-ray generator with a long fine focus sealed glass X-ray tube (PANalytical) was operated at 40 kV and 50 mA. A focusing multilayer optics and a block collimator provide an intense monochromatic primary beam (Cu-K_α, λ = 0.1542 nm). Samples were fixed and placed in a TCS 120 temperature-controlled unit (Anton Paar) along the line shaped X-ray beam in the evacuated camera housing. The sample-to-detector distance was 261.2 mm, and the temperature was kept at 26.0 °C. The 2D scattered intensity distribution recorded by an imaging-plate detector was read out by a Cyclone storage phosphor system (Perkin Elmer, USA). The 2D data were integrated into the one-dimensional scattering function $I(q)$ as a function of the magnitude of the scattering vector q defined as: $q = 4\pi \sin\theta/\lambda$, where λ is the wavelength and 2θ is the scattering angle. Each measurement was collected for 10 min. All $I(q)$ data were normalized to have the uniform primary intensity at q = 0 for transmission calibration. Desmearing is necessary because of the line collimation. Three times of repetition were performed.

2.6. Thermogravimetric analysis (TGA)

TGA data were collected using a PerkinElmer Pyris 1 TGA Thermogravimetric system (Perkin Elmer Inc., USA). The film samples were subjected to a heating rate of 10 °C/min in a heating range of 30–500 °C with Al_2O_3 as reference material. Nitrogen was used as the purge gas at a flow rate of 20 mL/min. Three times of repetition were performed.

2.7. Dynamic mechanical analysis (DMA)

DMA tests were carried out using a Pyris Diamond DMA (Perkin Elmer Inc., USA) under the tensile mode. The analyzer measured the complex tensile modulus E^*, *i.e.*, the storage component E' and the loss component E''. The ratio between the two components, $\tan\delta = E''/E'$, was also determined. In the present work, results are displayed through E' and $\tan\delta$. Measurements were performed at 1 Hz, and temperature was varied by steps of 2 °C between −100 and +200 °C.

2.8. Statistical analysis

All the data were subjected to one way analysis of variance and correlations between the result were carried out using Statistical Analysis System Software (SAS version 9.0, SAS Institute, Cary, NC); significant differences were determined by Duncan's multiple range test and accepted at $p < 0.01$ (Duncan, 1955).

3. Results and discussion

3.1. Morphological characteristics

The microscopic morphology of the cross-section of starch ester films was shown in Fig. 1. It is obvious that the cross-section of unplasticized film was rough, characterizing with the presence of white particles (Fig. 1a). However, the cross-section of plasticized film with 10 wt% triacetin presented different textures (Fig. 1b). The morphology was further changed by enhanced plasticizing effect

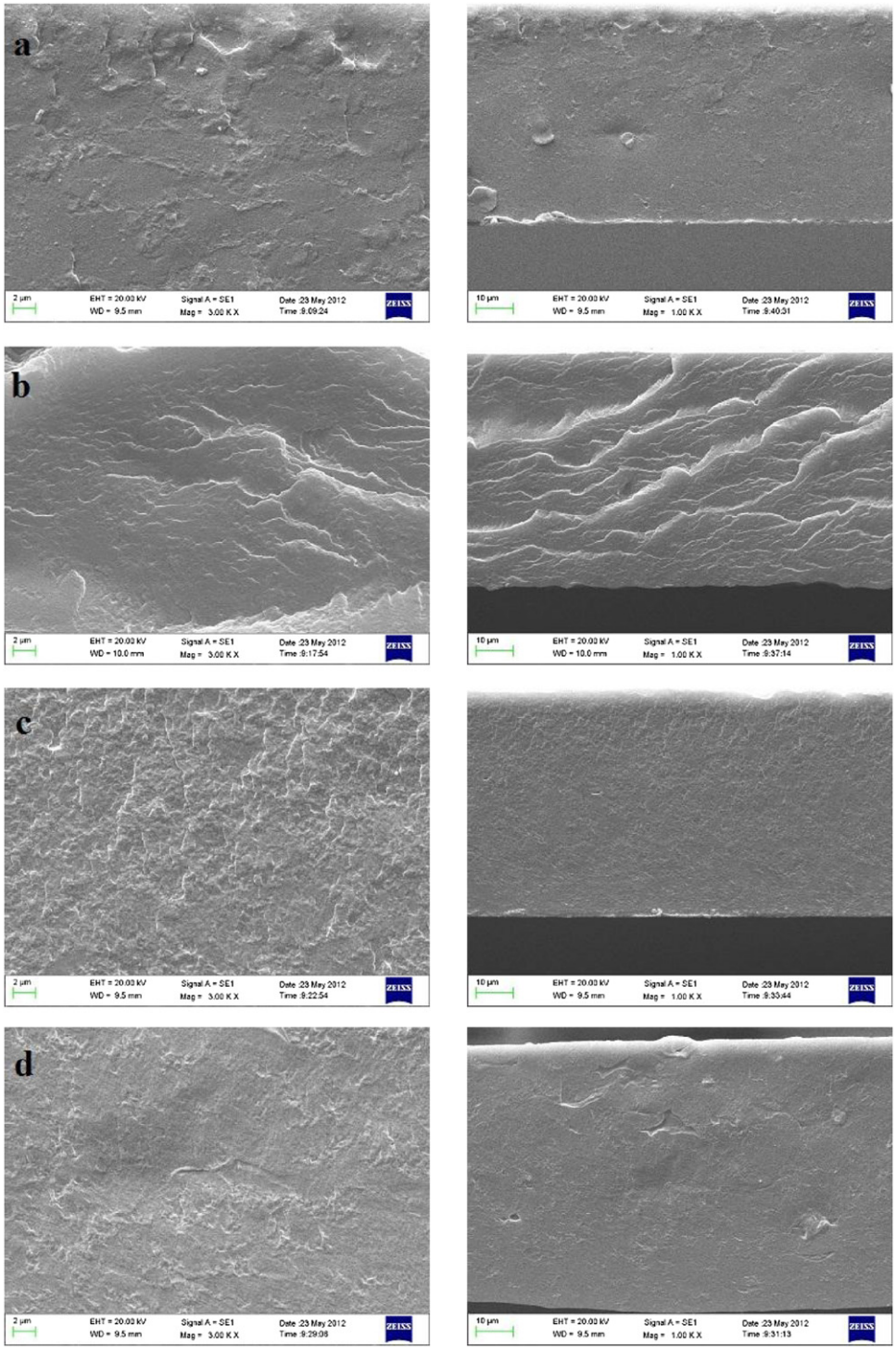

Fig. 1. SEM images of the cross-section of starch ester films with different triacetin contents (Left: 3000× magnification; Right: 1000× magnification). (a) 0 wt%, (b) 10 wt%, (c) 20 wt%, and (d) 30 wt%.

with more triacetin addition. Fig. 1(c) and (d) showed that the cross-section of plasticized films with more triacetin were of much less roughness without obvious particles or drape, which indicated that the plasticization could effectively promote the intuitive homogenization of the cross-section.

3.2. Interaction between plasticizer and starch ester molecules

When compounds are mixed, physical bonds and chemical interactions are reflected by changes in characteristic IR spectra peaks (Cerqueira, Souza, Teixeira, & Vicente, 2012). Fig. 2(a) shows the IR spectra of triacetin and starch ester films with/without triacetin. Compared with the film without triacetin, the IR spectrum of plasticized film presents new bands at *ca.* 1220 cm^{-1} and 1169 cm^{-1}, which were both attributed to the stretching vibration of ether bond (C—O) in alcoxyl group (C—O—C) of triacetin and starch ester molecules. By further deconvolution of these characteristic area bands (Fig. 2b), the changes of the peak position for plasticized films with different triacetin contents were presented in Fig. 2(c). With the increasing triacetin content, the bands at

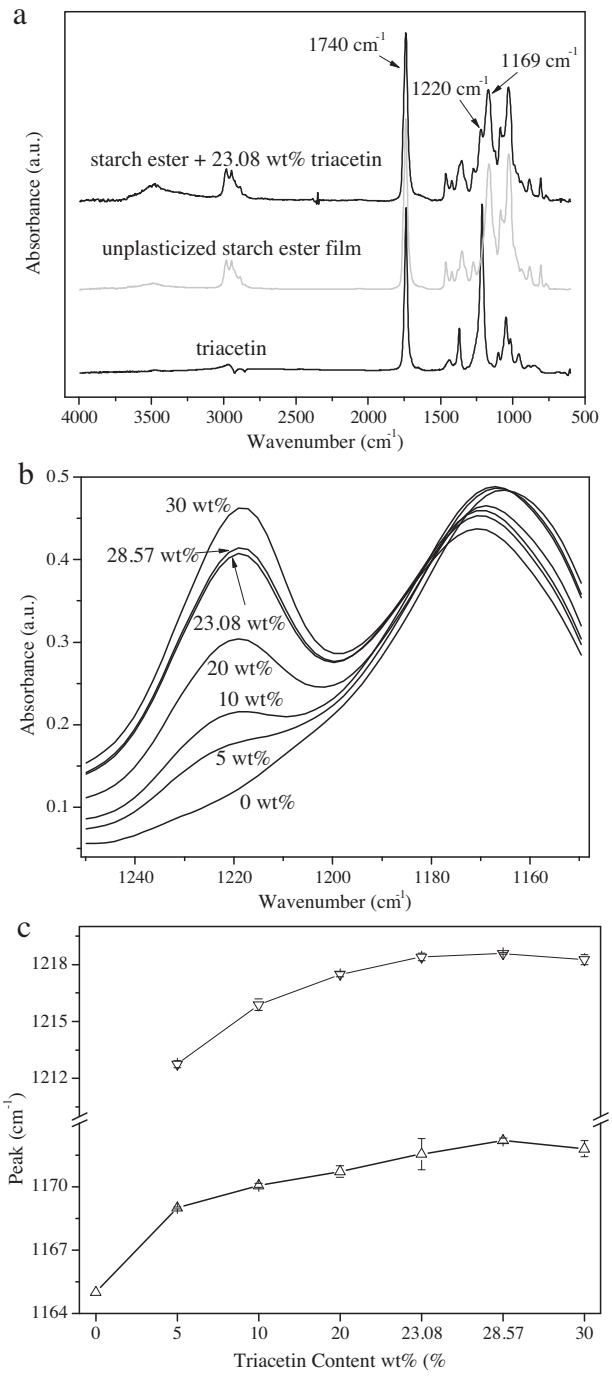

Fig. 2. (a) IR spectra of triacetin, unplasticized and plasticized starch ester films (The curves have been shifted vertically to avoid overlapping); (b) IR spectra between 1250 and 1150 cm^{-1} of plasticized starch ester films with different triacetin contents (The triacetin contents are indicated in the figure); (c) the variation of characteristic peaks from the stretching vibration of C—O in C—O—C bonds in plasticized films after deconvolution with Peak Fit 4.12.

1211 cm^{-1} and 1165 cm^{-1} gradually shifted to *ca.* 1219 cm^{-1} and 1172 cm^{-1} respectively, which indicated that the alcoxyl groups of both triacetin and starch ester molecules were enhanced. The gel theory (Santosa & Padua, 1999; Suyatma et al., 2005) considers that plasticizers take effect by breaking polymer–polymer interactions (*e.g.* hydrogen bonds and Van der Waals or ionic forces). According to the molecular structure of triacetin and starch ester, the primary inter- and intra-molecule forces in unplasticized and plasticized films are regarded as Van der Waals' force. Consequently, the

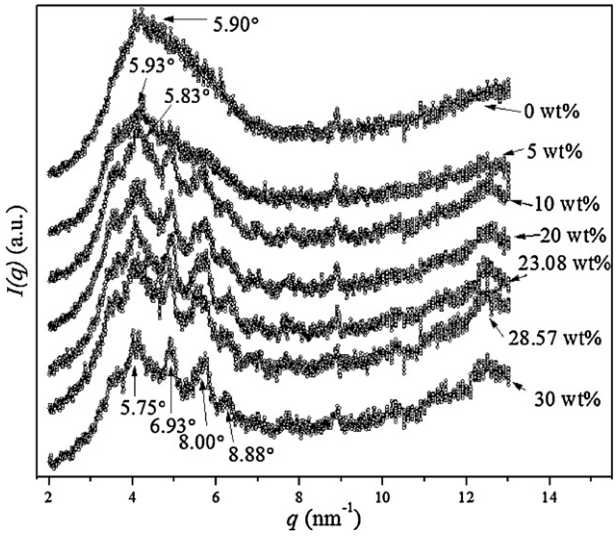

Fig. 3. WAXS data of starch ester films with different triacetin contents (The curves have been shifted vertically to avoid overlapping).

shifts of above-mentioned peaks should arise from the new intermolecular Van der Waals' force between triacetin and starch ester molecules. This new interaction replaced the respective molecular forces which originally belonged to triacetin and starch ester themselves. The gradually increasing interaction simultaneously weakened the original molecular forces.

3.3. Crystalline structure within the film matrix

Fig. 3 shows the WAXS patterns of starch ester films with/without triacetin. The diffractogram recorded for unplasticized starch ester film shows no diffraction peak and displays a typical behavior of fully amorphous polymer, which is characterized by a broad hump at around $2\theta = 5.90^\circ$ ($q = 4.2\ nm^{-1}$). For plasticized film with 5 wt% triacetin, several ill-defined peaks as well as the broad peak at $2\theta = 5.93^\circ$ were observed. With further increasing triacetin content, the amorphous broad hump was replaced by several well-defined diffraction peaks, which implied that new scattered crystallite formed in the film matrix. These result was reasonable since previous researches have also found the crystallization in other film systems plasticized with glycerol (Anglès & Dufresne, 2000; Cerqueira et al., 2012; Fabra, Talens, & Chiralt, 2010; Mathew & Dufresne, 2002). According to these researchers, the enhanced mobility of amorphous chains arising from plasticization facilitates the approach of chains to each other, thus the interaction among polymer chains is reinforced to form crystallite. To the best of our knowledge, more plasticizer increases polymer/plasticizer interaction and therefore decreases the interaction between macromolecule chains, which would hinder the crystallization. Mathew and Dufresne (2002) considered that the mild crystallization of hydrophilic starch could be boosted by plasticizers with high molecular weight, such as polyol, in dry atmosphere, or by plasticizers with low molecular weight in moist atmosphere. Considering the results and the hydrophobic property of starch ester and triacetin, consequently, we proposed that the crystallite could form in hydrophobic film matrix during plasticizing process. In addition, the peak at 5.83° (10 wt%) shifted to 5.75° (30 wt%) with increasing triacetin amount, indicating that the inter-planar spacing of associated crystallites was mild enlarged. For other three peaks representing smaller *d*-spacing at 6.93°, 8.00° and 8.88°, whereas no obvious changes was observed.

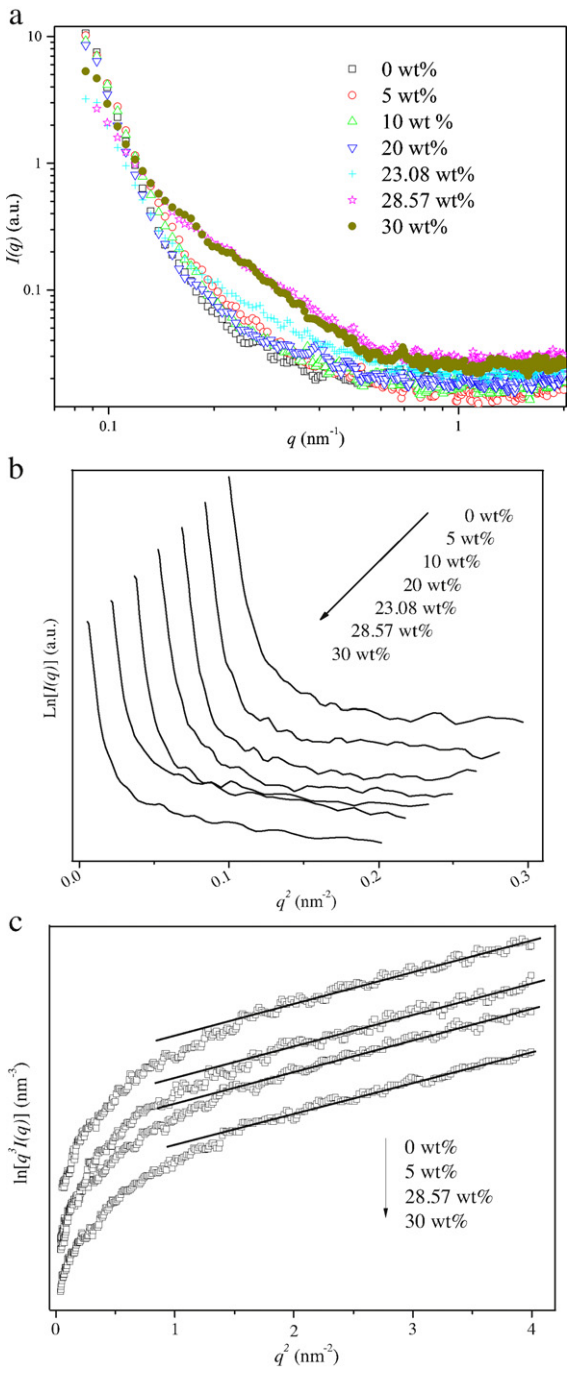

Fig. 4. (a) SAXS data of starch ester films with different triacetin contents plotted in the form of log[$I(q)$] *versus* log(q); (b) Guinier plot (ln[$I(q)$] *versus* q^2) (Waterfall from OriginPro 8); (c) positive deviation from Porod' law of SAXS data.

3.4. Microstructures and domain size

SAXS is powerful for analyzing not only the phase behaviors in condensed and solution states, but also the perturbed or nonperiodic structures of amorphous and mesormorphic materials (Chu & Hsiao, 2001; Doniach, 2001), which could provide the information about the overall shape and dimension of microphases (Baldini et al., 1999; Hilger & Stadler, 1992). The small angle scattering intensity is related to the electron density difference associated with nano-scale features within the films. Fig. 4(a) shows the difference of scattering intensity in small q regions which is expected to result from the triacetin incorporation. Known from the discussion above, scattered crystallites formed with the plasticizing effect, thus leading to more compact macromolecular chains with higher electron density in crystalline region than in amorphous part. Comparatively, despite no crystallite in unplasticized film, *i.e.* no electron density difference between such crystalline and amorphous region, apparent scattering intensity was still observed, from which it could be deduced that orderly region distribution with higher electron density existed in the amorphous unplasticized film.

For a two-component system, the scattering intensity can be then approximated by the equation below (Baldini et al., 1999):

$$I(q) = I(0)e^{-q^2R_g^2/3}$$

$I(0)$ is the scattering intensity at zero angle ($q = 0$) and R_g is the radius of gyration. For all samples, there is no maximum in the plots in Fig. 4(a), indicating existence of microphase separation in the films with no inter-particle interference (Chen & Zhang, 2005; Chen, Zhang, & Cao, 2005). All R_g values were estimated from the slope value of the regression line (Fig. 4b) according to Guinier equation $\ln[I(q)] = \ln[I(0)] - R_g^2q^2/3$ (Glatter & Kratky, 1982) and summarized in Table 2. For plasticized films, the R_g values, in the range from 34.0 to 36.6 nm, are slightly larger than that of unplasticized film ($p < 0.01$). The larger R_g value indicated that the crystalline structure, more or less, was expanded by triacetin to generate larger interspace, which agreed with the slightly increasing d value (WAXS result). The original distance between macromolecular chains in amorphous region, by comparison, was enlarged to more extent and the mobile space consequently increased for starch ester molecular chain.

SAXS curves plotted as $\ln[q^3I(q)] \sim q^2$ (Fig. 4c) show linearity with positive slope in large q-regions called positive deviation from Porod' law (Guinier & Fournet, 1955; Koberstein, Morra, & Stein, 1980). This behavior that polymers exhibit systematic deviations may be interpreted in terms of the detailed microstructure of the polymer. The positive deviation results from the presence of thermal density fluctuations or mixing within phases. It could be deduced from Fig. 4(c) that there were micro-regions with electron density fluctuation, *i.e.* inhomogeneous structure, existing in both unplasticized and plasticized films. These results indicated that starch ester chains rearranged non-uniform aggregation structure. Specially, some defect should exist in the crystalline structure.

3.5. Changes of thermal stability of plasticizer and film matrix

The changes of interaction and structure were supposed to further affect the thermal properties. Fig. 5 shows initial thermograms and the corresponding rate of thermal decomposition reaction (dw/dt) for triacetin, starch ester powder and starch ester films with/without triacetin. Two obvious peaks of weight loss were observed in the plots of starch ester films with the triacetin content from 5 wt% to 30 wt% (Fig. 5b). According to the thermal stability of triacetin, Peak 1 is related to the triacetin evaporation. The mild weight loss of starch ester powder and unplasticized film in the first step was attributed to the water evaporation process. Table 2 summarizes the Onset and peak values of thermal events in detail.

Interestingly, the thermal stability of triacetin significantly decreased (seen from Onset and peak values) after being mixed with starch ester. These two values of triacetin weight loss initially decreased from 108.69 °C and 157.09 °C (5 wt%) respectively to 80.05 °C and 124.32 °C (20 wt%) ($p < 0.01$), and subsequently increased to *ca.* 90 °C and 130 °C (28.57–30 wt%). As the triacetin evaporation was related to the destruction of molecular forces, the thermal stability of triacetin thus changed along with its interaction with starch ester molecules. Large proportion of triacetin molecular forces was replaced by the interaction with starch ester

Table 2
Peak values (°C) of thermal events from TGA; radius of gyration (R_g) (nm) from SAXS.

Samples	Triacetin	0 wt%	5 wt%	10 wt%	20 wt%	23.08 wt%	28.57 wt%	30 wt%	Starch powder
1st Peak	195.68 ± 1.24^{a}	–	157.09 ± 1.36^{b}	140.83 ± 0.72^{c}	124.32 ± 1.19^{f}	127.52 ± 0.52^{e}	132.79 ± 0.32^{d}	130.50 ± 1.24^{d}	–
2nd Peak	–	377.86 ± 1.05^{e}	380.66 ± 0.78^{d}	380.59 ± 0.71^{d}	381.5 ± 0.86^{cd}	383.93 ± 0.54^{b}	383.74 ± 0.96^{b}	383.07 ± 0.28^{bc}	385.69 ± 0.34^{a}
R_g	–	32.46 ± 0.36^{c}	34.31 ± 0.27^{ab}	34.03 ± 0.51^{b}	34.15 ± 0.87^{b}	36.59 ± 0.67^{a}	35.16 ± 0.44^{ab}	35.13 ± 0.29^{ab}	–

Superscript letters (a–f) indicate significant difference ($p < 0.01$) within the same row.

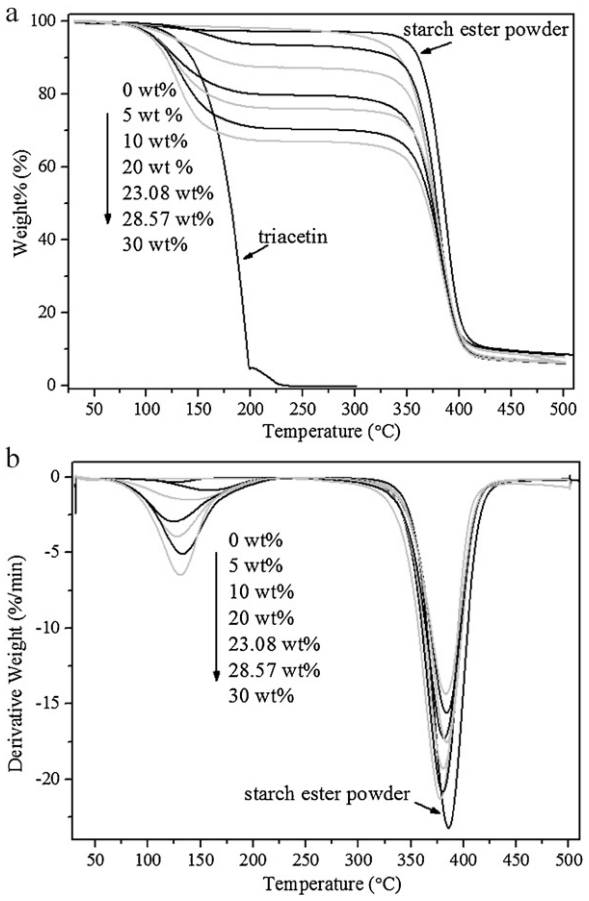

Fig. 5. TGA (a) and DTG (b) curves for starch ester films with different triacetin contents.

molecules when these two components were mixed. The triacetin within the film evaporated at lower temperature, from which it could be inferred that the intermolecular forces of triacetin were of higher stability than the interaction with starch ester. On the other hand, the increasing triacetin aggregated in the amorphous region to form plasticizer-rich domain because of the crystallization, which was also reported by Mathew and Dufresne (2002). The triacetin molecular forces should be much more remarkable within such amorphous region, which probably led to the subsequent increasing characteristic values of triacetin.

For the film matrix, Peak 2 is thought to be related with the depolymerization and pyrolytic decomposition of the polysaccharide backbone (Zohuriaan & Shokrolahi, 2004). Thermal analysis shows that unplasticized film was stable up to 343.67 °C (Onset value). All Onset and peak values increases in the order: unplasticized film < plasticized films < starch ester powder, which manifested that the plasticizing effect enhanced the thermal stability of starch ester film. The pyrolytic decomposition of starch ester film involves the depolymerization of macromolecular chains and the chemical bonds rupture. According to ATR-FTIR results, C—O—C of starch ester molecules was enhanced by plasticization. Although triacetin evaporated completely before the depolymerization and pyrolytic decomposition of the film matrix, however, on the other hand, the restriction from crystallite reduced the thermal motion of macromolecular chains. Further, compared with the spread chains in the film, the molecular chains curl within the starch ester granules presenting the most stable thermal property, which proves that the restriction on chain mobility could enhance the thermal stability.

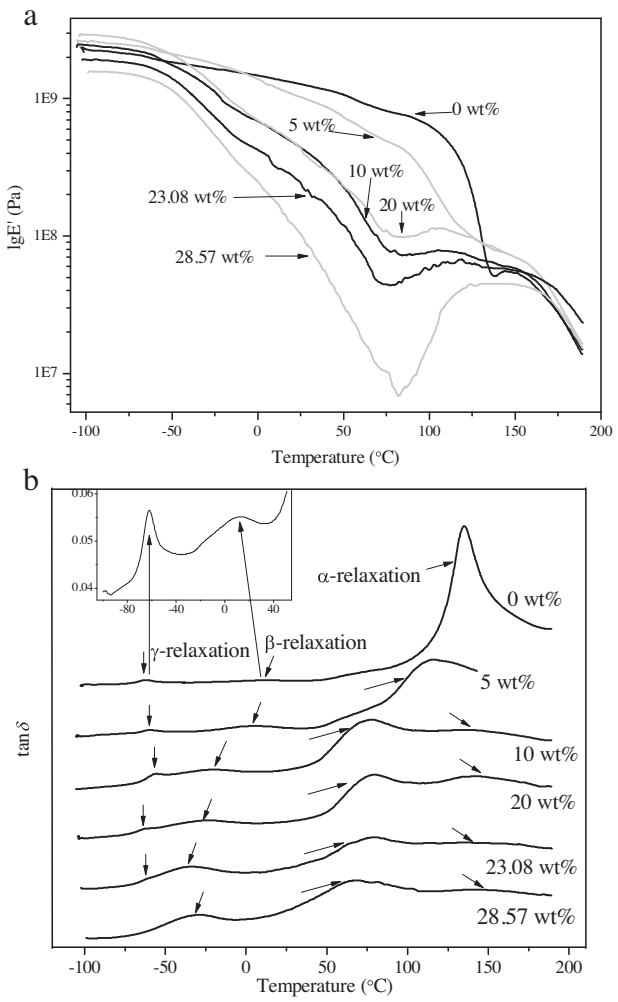

Fig. 6. (a) Logarithm of the storage tensile modulus E' and (b) loss angle tangent $\tan\delta$ on a liner scale *versus* temperature for starch ester films with different triacetin contents (The inset stands for the amplification of unplasticized film curve for distinguishing). The curves have been shifted vertically for clarity.

From the results of FTIR and thermal analysis we speculate that the interaction between triacetin and starch ester molecules display less stability than the molecular forces that belongs to respective molecules. However, this interaction is essential to film forming but unexpectedly lowers the thermal property of triacetin in such film matrix.

3.6. Relaxation behaviors

Fig. 6 shows the isochronal plot of log E' (storage tensile modulus, Fig. 6a and $\tan\delta$ (loss angle tangent, Fig. 6b). Below −40 °C, E' presented mild difference between the film materials. However, an overall decrease of E' with increasing triacetin content could be observed. Moreover, E' also decreased more in the range of −40 to 100 °C. This decrease should result from the energy dissipation phenomena involving cooperative motions of long amorphous sequences within different surroundings (Anglès & Dufresne, 2001). The correlation between the decrease degree of E' and triacetin content indicated that more triacetin endowed the macromolecular chains in the plasticized films with higher flexibility (*i.e.* mobility). The similarity between the sample curves (10 wt% and 20 wt% contents) are most probably attributed to simultaneous effect from the different amount of crystallite and triacetin contents. Above 75 °C, we observe an E' increase for the film materials with triacetin content from 10 wt% to 28.57 wt%. According to TGA results, triacetin evaporated above 75 °C, thus the improvement to chains mobility was weakened.

The concomitant relaxation progresses are shown in Fig. 6(b). Unplasticized starch ester film in the range −100 to 200 °C showed three relaxations. The visible γ-relaxation (low activation energy and characteristic time value of the same order as Debye time) (Fringant et al., 1998) around −62 °C corresponded to the local non-cooperative motion of the side groups, *i.e.* substitution group or non-substituted hydroxyl, in the amorphous phase. This relaxation gradually disappeared with the increasing triacetin content and along with the appearance of the adjacent β-relaxation to be precise. It is also possible because of the anti-plasticization of crystallite domain.

The unconspicuous β-relaxation around 14 °C (see the inset in Fig. 6b), which reflects the significantly cooperative motion within unplasticized film, was enhanced with the increasing triacetin content. The peak temperature obviously decreased from 14 °C (0 wt%) to −30 °C (28.57 wt%). Other researchers have attributed this relaxation at low temperature (around −50 °C to −40 °C) to the glass–rubber transition of "plasticizer (glycerol)-rich" domain in their film matrix (Angellier, Molina-Boisseau, Dole, & Dufresne, 2006; Anglès & Dufresne, 2000, 2001; Chen & Zhang, 2005; Mathew & Dufresne, 2002). In previous studies, the relaxation in DMA or new heat increment in DSC at low temperature only appeared for plasticized films with high glycerol content (generally more than 20%). Moreover, only a single glass–rubber transition for films plasticized with the same content of other polyols was detected, of which the molecular weight is twice or more than glycerol (Mathew & Dufresne, 2002). That is to say, plasticized starch films with high glycerol content resulted in the phase separation with glycerol-rich and amylopectin-rich domains. The β-relaxation observed in starch ester films both with and without triacetin has also been reported in previous research (Fringant et al., 1998). The authors considered a phase separation and a system with two glass transition temperatures. This relaxation in our research would reflect the phase transition of the short molecular chains within the most plasticized part, *i.e.* the amorphous region with the enrichment of squeezed triacetin from crystallite.

The α-relaxation relevant to the cooperative motion of molecular chains in ultra-nanometer scale is the glass–rubber transition. The $\tan\delta$ peak value of α-relaxation decreased from *ca.* 135 °C to 70 °C after triacetin incorporation, indicating that the plasticization effectively lowered the glass–rubber transition temperature. However, the peak value displayed no obvious changes with further increasing triacetin content (≥10 wt%). This most probably resulted from the two opposite effects: plasticization from more triacetin and anti-plasticization from crystalline domains which act as cross-links and restrict the relaxation of the amorphous amylopectin regions (Mathew & Dufresne, 2002). In addition, the intensity of $\tan\delta$ peak decreased obviously and the half-height width increased. Anglès and Dufresne (2001) have previously reported that the intensity mainly depends on the magnitude of the modulus drop, while the half-height width stands for the size distribution of mobile entities participating in the relaxation. These changes most probably resulted from the crystallite formation in the film since the similar discussion has been reported (Anglès & Dufresne, 2001). Interestingly, new peaks at 133 °C, 142 °C, 135 °C and 141 °C were detected for the films with 10 wt%, 20 wt%, 23.08 wt% and 28.57 wt% triacetin content, which could be related to the lamellar slip mechanism and also rotation within crystals (Bikiaris, Matzinos, Larena, Flaris, & Panayiotou, 2001; Manchado, Valentini, Biagiotti, & Kenny, 2005; Razavi-Nouri, 2012). Although we raised the heating temperature to 250 °C, this relaxation did not appear for 0 wt% and 5 wt% samples. The different definition of this peak was supposed to associate with the different crystallinity within films. Although we

proposed that most triacetin was squeezed from crystalline region in before-mentioned conclusion, plasticizing effect still affected this new relaxation relating to the crystalline structure. It is worth further noting that the chains motion in different scale could depend on molecular weight distribution.

4. Conclusions

Triacetin as plasticizer affected multiple structures and properties of starch ester film. The triacetin incorporation enhanced C—O in C—O—C of starch ester molecule and facilitated the crystallite formation. The distance between macromolecular chains and the whole amorphous region was enlarged by more triacetin molecules squeezed from crystalline region, consequently, which increased the free volume and the chain motions. The enhanced C—O and the restriction from crystalline structure on the mobility of macromolecular chain improved the thermal property of film matrix. The thermal stability of triacetin within the film matrix changed due to the fluctuant interaction with starch ester molecules. The higher flexibility of macromolecular chain aggravated the decrease of storage tensile modulus along with heating and promoted the relaxation in different scale, including the side groups, short molecular chains and ultra-nanometer scale. However, the crystallite exerted restriction on these viscoelastic behaviors. The size distribution of mobile entities participating in the glass–rubber transition was affected by different microstructures within the film matrix. The structure–property relation should contribute to the further structure modification and applications in different environment, such as processing temperature, of such hydrophobic biodegradable packaging materials.

Acknowledgements

The authors would like to acknowledge the National Natural Science Funds of China (No. 21076086, 31130042), the National Key Technology R&D Program (2012BAD37B01, 2012BAD34B07) and National Program on Key Basic Research Project (2012CB720801).

References

Angellier, H., Molina-Boisseau, S., Dole, P., & Dufresne, A. (2006). Thermoplastic starch-waxy maize starch nanocrystals nanocomposites. *Biomacromolecules*, *7*, 531–539.

Anglès, M. N., & Dufresne, A. (2000). Plasticized starch/tunicin whiskers nanocomposites. 1. Structural analysis. *Macromolecules*, *33*, 8344–8353.

Anglès, M. N., & Dufresne, A. (2001). Plasticized starch/tunicin whiskers nanocomposite materials. 2. Mechanical behavior. *Macromolecules*, *34*, 2921–2931.

Avérous, L., & Halley, P. J. (2009). Biocomposites based on plasticized starch. *Biofuels Bioproducts and Biorefining – Biofpr*, *3*, 329–343.

Baldini, G., Beretta, S., Chirico, G., Franz, H., Maccioni, E., Mariani, P., et al. (1999). Salt-induced association of β-lactoglobulin by light and X-ray scattering. *Macromolecules*, *32*, 6128–6138.

Bikiaris, D., Matzinos, P., Larena, A., Flaris, V., & Panayiotou, C. (2001). Use of silane agents and poly(propylene-g-maleic anhydride) copolymer as adhesion promoters in glass fiber/polypropylene composites. *Journal of Applied Polymer Science*, *81*, 701–709.

Bonacucina, G., Di Martino, P., Piombetti, M., Colombo, A., Roversi, F., & Palmieri, G. F. (2006). Effect of plasticizers on properties of pregelatinised starch acetate (Amprac 01) free films. *International Journal of Pharmaceutics*, *313*, 72–77.

Cerqueira, M. A., Souza, B. W. S., Teixeira, J. A., & Vicente, A. A. (2012). Effect of glycerol and corn oil on physicochemical properties of polysaccharide films – A comparative study. *Food Hydrocolloids*, *27*, 175–184.

Chandra, R., & Rustgi, R. (1998). Biodegradable polymers. *Progress in Polymer Science*, *23*, 1273–1335.

Chen, P., & Zhang, L. (2005). New evidences of glass transitions and microstructures of soy protein plasticized with glycerol. *Macromolecular Bioscience*, *5*, 237–324.

Chen, P., Zhang, L., & Cao, F. (2005). Effects of moisture on glass transition and microstructure of glycerol-plasticized soy protein. *Macromolecular Bioscience*, *5*, 872–880.

Chen, L., Li, X. X., Li, L., & Guo, S. Y. (2007). Acetylated starch-based biodegradable materials with potential biomedical applications as drug delivery systems. *Current Applied Physics*, *7S1*, e90–e93.

Chu, B., & Hsiao, B. S. (2001). Small-angle X-ray scattering of polymers. *Chemical Reviews*, *101*, 1727–1761.

Doniach, S. (2001). Changes in biomolecular conformation seen by small angle X-ray scattering. *Chemical Reviews*, *101*, 1763–1778.

Duncan, D. B. (1955). Multiple range and multiple F test. *Biometrics*, *11*, 1–42.

Fabra, M. J., Talens, P., & Chiralt, A. (2010). Water sorption isotherms and phase transitions of sodium caseinate-lipid films as affected by lipid interactions. *Food Hydrocolloids*, *24*, 384–391.

Fringant, C., Rinaudo, M., Foray, M. F., & Bardet, M. (1998). Preparation of mixed esters of starch or use of an external plasticizer: Two different ways to change the properties of starch acetate films. *Carbohydrate Polymers*, *35*, 91–106.

Glatter, O., & Kratky, O. (1982). *Small angle X-ray scattering*. London, UK: Academic Press., pp. 119–196.

Guinier, A., & Fournet, G. (1955). *Small-angle scattering of X-rays*. New York, USA: Wiley., p. 268.

Hilger, C., & Stadler, R. (1992). Cooperative structure formation by directed noncovalent interactions in an unpolar polymer matrix. 7. Differential scanning calorimetry and small-angle X-ray scattering. *Macromolecules*, *25*, 6670–6680.

Koberstein, J. T., Morra, B., & Stein, R. S. (1980). The determination of diffuse-boundary thickness of polymers by small angle X-ray scattering. *Journal of Applied Crystallography*, *13*, 34–45.

Manchado, M. A. L., Valentini, L., Biagiotti, J., & Kenny, J. M. (2005). Thermal and mechanical properties of single-walled carbon nanotubes–polypropylene composites prepared by melt processing. *Carbon*, *43*, 1499–1505.

Mathew, A. P., & Dufresne, A. (2002). Plasticized waxy maize starch: Effect of polyols and relative humidity on material properties. *Biomacromolecules*, *3*, 1101–1108.

Matveev, Y. I., Grinberg, V. Y., & Tolstoguzov, V. B. (2000). The plasticizing effect of water on proteins, polysaccharides and their mixtures. Glassy state of biopolymers, food and seeds. *Food Hydrocolloids*, *14*, 425–437.

Nejad, M. H., Ganster, J., & Volkert, B. (2010). Starch esters with improved mechanical properties through melt compounding with nanoclays. *Journal of Applied Polymer Science*, *118*, 503–510.

Nejad, M. H., Ganster, J., Bohn, A., Volkert, B., & Lehmann, A. (2011). Nanocomposites of starch mixed esters and MMT: Improved strength, stiffness, and toughness for starch propionate acetate laurate. *Carbohydrate Polymers*, *84*, 90–95.

Pu, H. Y., Chen, L., Li, X. X., Xie, F. W., Yu, L., & Li, L. (2011). An oral colon-targeting controlled release system based on resistant starch acetate: Synthetization, characterization, and preparation of film-coating pellets. *Journal of Agricultural and Food Chemistry*, *59*, 5738–5745.

Rapthel, I., Wagner, B., & Kakuschke, R. (1998). Investigation of the plasticizing effect of dicarboxylic acid diesters on starch acetate. *Journal of Thermal Analysis*, *52*, 157–164.

Razavi-Nouri, M. (2012). Effect of carbon nanotubes on dynamic mechanical properties, TGA, and crystalline structure of polypropylene. *Journal of Applied Polymer Science*, *124*, 2541–2549.

Santosa, F. X. B., & Padua, G. W. (1999). Tensile properties and water absorption of zein sheets plasticized with oleic and linoleic acids. *Journal of Agricultural and Food Chemistry*, *47*, 2070–2074.

Shogren, R. (1992). Effect of moisture content on the melting and subsequent physical aging of corn starch. *Polymer*, *19*, 83–90.

Siracusa, V., Rocculi, P., Romani, S., & Rosa, M. D. (2008). Biodegradable polymers for food packaging: A review. *Trends in Food Science and Technology*, *19*, 634–643.

Suyatma, N. E., Tighzert, L., Copinet, A., & Coma, V. (2005). Effects of hydrophilic plasticizers on mechanical, thermal, and surface properties of chitosan films. *Journal of Agricultural and Food Chemistry*, *53*, 3950–3957.

Tarvainen, M., Sutinen, R., Peltonen, S., Mikkonen, H., Maunus, J., Vähä-Heikkilä, K., et al. (2003). Enhanced film-forming properties for ethyl cellulose and starch acetate using n-alkenyl succinic anhydrides as novel plasticizers. *European Journal of Pharmaceutical Sciences*, *193*, 63–371.

Tharanathan, R. N. (2003). Biodegradable films and composite coatings: Past, present and future. *Trends in Food Science and Technology*, *14*, 71–78.

Viera, M. G. A., Da Silva, M. A., Dos Santos, L. O., & Beppu, M. M. (2011). Natural-based plasticizers and biopolymer films: A review. *European Polymer Journal*, *47*, 254–263.

Volkert, B., Lehmann, A., Greco, T., & Nejad, M. H. (2010). A comparison of different synthesis routes for starch acetates and the resulting mechanical properties. *Carbohydrate Polymers*, *79*, 571–577.

Zohuriaan, M. J., & Shokrolahi, F. (2004). Thermal studies on natural and modified gums. *Polymer Testing*, *23*, 575–579.